Development of a New Generic Analytical Modeling of AC Coupling Losses in Cable-in-Conduit Conductors

Alexandre Louzguiti, Louis Zani, Daniel Ciazynski, Bernard Turck, Jean-Luc Duchateau, Alexandre Torre, Frédéric Topin, Marco Bianchi, Anna Chiara Ricchiuto, Tommaso Bagni, Valiyaparambil Abdulsalam Anvar, Arend Nijhuis, and Ion Tiseanu

***Abstract*—Coupling losses induced in cable-in-conduit conductors (CICC) when subject to a time-varying magnetic field are a major issue commonly encountered in large fusion tokamaks (e.g., JT-60SA, ITER, DEMO). The knowledge of these losses is crucial to determine the stability of CICC but is yet difficult to achieve analytically (thus in a short computation time) given the specific and complex architecture of these conductors although numerical solutions such as THELMA and JACKPOT already exist. In an attempt to ease the resolution of this problem, we have previously presented a theoretical generic study of a group of elements twisted together (representing a cabling stage of a CICC) and derived the analytical expression of its coupling losses. We have now extended this study to a two cabling stage conductor by establishing an analytical model to calculate its coupling losses as function of its effective features. In a second part, we compare our results to these of THELMA and JACKPOT on geometries representing ITER CS and JT-60SA TF conductors. Finally, we have set up a specific algorithm to reconstruct strand trajectories from X-ray images and have extracted the effective geometrical parameters of a JT-60SA TF conductor. Our next objective is then to extract its effective electrical parameters from interstrand resistivity measurements to be able to compare the coupling losses predicted by our analytical model with those measured within the SULTAN facility.**

***Index Terms*—AC losses, analytical, superconducting, transient regimes, effective parameters.**

Manuscript received August 29, 2017; accepted January 3, 2018. Date of publication January 12, 2018; date of current version February 1, 2018. This work was supported in part by the Conseil Régional Provence-Alpes-Côte d'Azur, and in part by the ASSYSTEM. *(Corresponding author: Alexandre Louzguiti.)*

A. Louzguiti is with the Commissariat à l'Energie Atomique et aux Energies Alternatives, CEA/DRF/IRFM, CEA Cadarache, Saint-Paul-lès-Durance 13108, France, and also with the Aix-Marseille Université, CNRS, IUSTI UMR 7343, Marseille 13453, France (e-mail: alexandre.mehdi.louzguiti@cern.ch).

L. Zani, D. Ciazynski, B. Turck, J.-L. Duchateau, and A. Torre are with the Commissariat à l'Energie Atomique et aux Energies Alternatives, CEA/DRF/IRFM, CEA Cadarache, Saint-Paul-lès-Durance 13108, France.

F. Topin is with the Aix-Marseille Université, CNRS, IUSTI UMR 7343, Marseille 13453, France.

M. Bianchi and A. C. Ricchiuto are with the Department of Electrical Engineering, University of Bologna, Bologna 40136, Italy.

T. Bagni, V. A. Anvar, and A. Nijhuis are with the University of Twente, Enschede 7522, The Netherlands.

I. Tiseanu is with the Institutul National pentru Fizica Laserilor, Plasmei si Radiatiilor, Bucharest 077125, Romania.

Color versions of one or more of the figures in this paper are available online at http://ieeexplore.ieee.org.

Digital Object Identifier 10.1109/TASC.2018.2792487

I. Introduction

COUPLING losses are a phenomenon occurring when a composite conductor (i.e., made of resistive and superconducting parts) is subject to a time-varying magnetic field. They can be seen as a type of eddy currents but they are largely influenced by the trajectories of the superconducting parts of the conductor. For a multifilamentary composite experiencing the time variation of a transverse and uniform magnetic field, the combined work of the community [1]–[8] has provided a useful and simple analytical modeling commonly summarized [9], [10] by the equation

$$B_{\mathrm{int}} + \tau \dot{B}_{\mathrm{int}} = B_a \tag{1}$$

where B_{int} is the induction inside the composite (the overdot notation represents the time derivative), B_a is the applied magnetic field and τ is the time constant of the coupling currents. The associated formula of instant power dissipated per unit volume of filamentary zone (cylinder enclosed by the outer ring of superconducting filaments) is

$$P = 2\tau \dot{B}_{\mathrm{int}}^2 / \mu_0 \tag{2}$$

Its integration over a cycle of a sinusoidal magnetic excitation $B_a = B_p \sin(\omega t)$ leads to

$$Q(\omega) = \frac{B_p^2}{\mu_0} \frac{2\pi\omega\tau}{1 + (\omega\tau)^2} \tag{3}$$

For conductors with a more sophisticated design, it is very difficult to analytically solve the diffusion equation governing the coupling currents as the geometry can be very challenging. In addition several studies [11]–[15] have shown that the single time constant approach fails at describing the conductor response to an arbitrary time-varying magnetic field. The Multizone PArtial Shielding (MPAS) model [16] has then proposed a heuristic approach which assumes that, in a CICC with *N* cabling stages, the energy dissipated over a cycle of a sinusoidal magnetic excitation $B_a = B_p \sin(\omega t)$ per unit volume of cable envelope can be expressed as

$$Q(\omega) = \frac{B_p^2}{\mu_0} \sum_{j=1}^{N} \frac{n\kappa_j \pi\omega\theta_j}{1 + (\omega\theta_j)^2} \tag{4}$$

Indeed, MPAS considers that in a CICC, the magnetic shielding can in the end be represented with a set of magnetically decoupled zones, each featuring a time constant θ_j and a coefficient $n\kappa_j$ accounting for its effective shielding. Note that, in this approach, the $n\kappa_j$ and θ_j must be determined from coupling losses measurements following a specific methodology and that they include shielding effects from the different cabling stages; for further details on MPAS, the reader is referred to [16].

Our objective is to provide an analytical model able to predict the coupling losses dissipated in a CICC from its geometrical and electrical features (e.g., able to predict the $n\kappa_j$ and θ_j considered in MPAS). Therefore, we have started by theoretical generic studies of the losses generated inside composites featuring complex geometries [17] and inside a group of twisted elements [18]. In the latter one, we have demonstrated that the magnetic shielding made by a group of elements can exactly be represented as in the MPAS model and we have derived the analytical expressions of its time constant θ and its coefficient $n\kappa$. We have chosen to express the losses under this specific form because we value its simplicity: it allows an enlightening physical interpretation of the shielding made by a CICC, it can rapidly be integrated into multiphysics platforms and can provide fair results with very low CPU consumption.

More recently, we have studied the magnetic shielding occurring in a two cabling stage conductor and have found a method to compute its time constants θ_j and their associated coefficients $n\kappa_j$ as functions of its effective electrical and geometrical features. We will therefore present here the guidelines of our model and the results of its comparisons with reference numerical models.

II. Analytical Modeling

We represent two cabling stages of a conductor as N_2 bundles of N_1 elements. The advantage of this approach is that the scale of the element is not fixed: indeed the element can represent a strand or a sub-petal. In fact, our strategy is to represent the dynamics of shielding between two consecutive stages regardless of the scale.

A. Assumptions

The elements of the conductor are represented by a superconducting tube surrounded by copper (see Fig. 1) and are lightly twisted, i.e., $(2\pi R_{c_1}/l_{p_1})^2 \ll 1$ and $(2\pi R_{c_2}/l_{p_2})^2 \ll 1$. R_{c_1}, R_{c_2} are the cabling radii of the two stages, and l_{p_1}, l_{p_2} their respective twist pitches with $l_{p_2} \neq k l_{p_1}$ $(k \in \mathbb{Z})$; the system is thus not periodic. We consider that the superconducting tubes are not saturated to avoid any nonlinearity, i.e., they have zero longitudinal resistance. The applied magnetic field B_a is along the y-axis and spatially uniform. The only other magnetic contribution we consider is the one generated by the induced currents flowing through the superconducting tubes and we assume its axial component to be negligible because the elements are lightly twisted. We consider an effective transverse conductance per unit length of conductor which is constant and different for each scale: σ_{l_1} between adjacent elements and σ_{l_2} between adjacent bundles of elements.

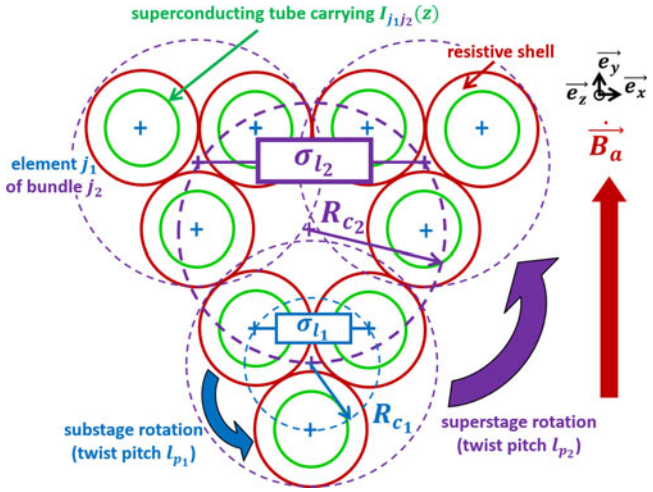

Fig. 1. Cross-section of a triplet of triplets along with transverse conductances.

B. Equations

Given the complexity of the calculations, they will not be exhaustively detailed here. Alternatively, we will present the baseline of our approach in this section.

The superconducting tube of the element j_1 of bundle j_2 carries a current $I_{j_1 j_2}$ which depends on z and flows mainly in the axial direction (light twisting of the elements); we decompose it as $I_{j_1 j_2} = I^{(1)}_{j_1 j_2} + I^{(2)}_{j_2}/N_1$ where $I^{(1)}_{j_1 j_2}$ is the current shielding the substage scale and $I^{(2)}_{j_2}$ is the one shielding the superstage scale. As in other analytical approaches (e.g., [19]), we have used Faraday's law of induction and Kirchhoff's current law to derive the equations governing the $I^{(1)}_{j_1 j_2}$ and $I^{(2)}_{j_2}$; we have then combined these equations to obtain the following equations on the $I_{j_1 j_2}$ (written in complex notations)

$$\begin{aligned}
&\frac{d^2 I_{j_1 j_2}}{dz^2} - \sigma_{l_1}\left(2\dot{A}_{z_{r\,j_1 j_2}} - \dot{A}_{z_{r\,j_1-1 j_2}} - \dot{A}_{z_{r\,j_1+1 j_2}}\right) \\
&- \left(\sigma_{l_2}/N_1^2\right)\sum_{k_1=1}^{N_1}\left(2\dot{A}_{z_{r\,k_1 j_2}} - \dot{A}_{z_{r\,k_1 j_2-1}} - \dot{A}_{z_{r\,k_1 j_2+1}}\right) \\
&= -4\dot{B}_a \sigma_{l_1} R_{c_1} \sin^2(\pi/N_1)\, e^{i\alpha_1 z} e^{i2\pi(j_1-1)/N_1} \\
&\quad - 4\dot{B}_a\left(\sigma_{l_2}/N_1\right) R_{c_2} \sin^2(\pi/N_2)\, e^{i\alpha_2 z} e^{i2\pi(j_2-1)/N_2} \qquad (5)
\end{aligned}$$

with $\alpha_1 = 2\pi/l_{p_1}$ and $\alpha_2 = 2\pi/l_{p_2}$. $A_{z_{r\,j_1 j_2}}$ is the magnetic vector potential at the center of element j_1 of bundle j_2 which is due to all the induced currents; it thus contains the inductive information of the system. To obtain an equation on the induced currents only, we have to explicitly express the dependence of $A_{z_{r\,j_1 j_2}}$ on the $I_{j_1 j_2}$ using Biot-Savart law; the problem is that this law requires the knowledge of the variations of the $I_{j_1 j_2}$ with z. To tackle this issue, we have used an iterative analytical reasoning along with Fourier expansion; this has enabled us to derive the following solution

$$I_{j_1 j_2}(z,t) = \sum_{k=-\infty}^{+\infty} I_0^{(\alpha_k)}(t)\cos\left(\alpha_k z + \varphi^{(k)}_{j_1 j_2}\right) \qquad (6)$$

where $I_0^{(\alpha_k)}$ is an amplitude depending on time only, $\varphi_{j_1 j_2}^{(k)}$ is an initial phase and α_k is a spatial frequency given by

$$\alpha_k = \alpha_1 + (k-1)(\alpha_2 - \alpha_1), k \in \mathbb{Z} \tag{7}$$

Injecting (6) into (5), we actually obtain an infinite system of time equations on the $I_0^{(\alpha_k)}$: it thus cannot be solved. However, we have computed the response of two different conductors (respectively representing the first and last two cabling stages of JT-60SA TF CICC) to a step function of B_a and have observed a very fast exponential decay of the magnetic coupling between the $I_0^{(\alpha_k)}$ amplitudes with increasing $|k-3/2|$: indeed, for $k<0$ and $k>3$, the $I_0^{(\alpha_k)}$ amplitudes were largely negligible compared to the others. It is therefore possible to consider only the amplitudes associated with these four spatial frequencies: $\{\alpha_0 = 2\alpha_1 - \alpha_2\ ; \alpha_1\ ; \alpha_2\ ; \alpha_3 = 2\alpha_2 - \alpha_1\}$. This simplification has enabled us to reduce the infinite matrix equation to the following one

$$\begin{bmatrix} I_0^{(\alpha_0)} \\ I_0^{(\alpha_1)} \\ I_0^{(\alpha_2)} \\ I_0^{(\alpha_3)} \end{bmatrix} + \begin{bmatrix} \tau_{11} & \tau_{12} & 0 & 0 \\ \tau_{21} & \tau_{22} & \tau_{23} & 0 \\ 0 & \tau_{32} & \tau_{33} & \tau_{34} \\ 0 & 0 & \tau_{43} & \tau_{44} \end{bmatrix} \begin{bmatrix} \dot{I}_0^{(\alpha_0)} \\ \dot{I}_0^{(\alpha_1)} \\ \dot{I}_0^{(\alpha_2)} \\ \dot{I}_0^{(\alpha_3)} \end{bmatrix} = \begin{bmatrix} 0 \\ y_{1\,\mathrm{ext}} \\ y_{2\,\mathrm{ext}} \\ 0 \end{bmatrix} \dot{B}_a \tag{8}$$

where $y_{k\,\mathrm{ext}} = 4R_{c_k}(\sigma_{l_k}/N_1^{k-1})\sin^2(\pi/N_k)/\alpha_k^2$ for $k=1$ or 2. The expressions of the time coefficients are rather complex [20] and are thus not detailed here. They depend on the effective transverse conductances per unit length of conductor (σ_{l_1} and σ_{l_2}) and feature non-elementary integrals which depends only on the geometrical parameters of the conductor and can be evaluated numerically in a very short time.

In addition, we have derived the instant coupling power per unit length of conductor as follows

$$P_l = N_1 N_2 \sum_{k=0}^{3} \frac{\left[\alpha_k I_0^{(\alpha_k)}\right]^2}{\gamma_k} \tag{9}$$

where $\gamma_0 = 32\sigma_{l_1}\sin^2(\pi/N_1)\cos^2(\pi/N_1)$, $\gamma_1 = \gamma_3 = 8\sigma_{l_1}\sin^2(\pi/N_1)$ and $\gamma_2 = 8\sigma_{l_2}\sin^2(\pi/N_2)/N_1$. The presence of σ_{l_1} in γ_0, γ_1 and γ_3 clearly indicates that α_0, α_1 and α_3 are spatial frequencies due to the magnetic shielding made by the substage scale while α_2 is due to the superstage scale.

Finally, we have also shown that the θ_j considered in MPAS are in fact the eigenvalues of the matrix of (8) and we have established a method to determine their associated coefficients $n\kappa_j$ [20] from (8) and (9). This result is important as we have demonstrated the origin of (4) which, until now, was a heuristic assumption considered by MPAS. The only difference is the number of time constants (remaining after simplification) in both models: two in MPAS and four in ours for a two cabling stages conductor.

TABLE I
EFFECTIVE PARAMETERS EXTRACTED FROM THELMA DATA

Effective parameters	l_{p_k} (mm)	R_{c_k} (mm)	σ_{l_k} (10^7 S/m)
Substage ($k=1$))	112.5	3.86	2.36
Superstage ($k=2$)	450.0	11.49	6.50

III. COMPARISON WITH NUMERICAL MODELS

We now consider that our analytical approach has reached a sufficient level of maturity to compare it with reference numerical models (THELMA and JACKPOT); we present the outputs of these comparisons in this section. We have used Fourier transforms on the element trajectories generated by each code to extract the effective cabling radii and twist pitches and we have averaged the conductances between adjacent elements of the same bundle to obtain σ_{l_1} and between adjacent bundles to obtain σ_{l_2}. We have here chosen a simple but physically realistic method to obtain the effective parameters needed in our analytical model; note that other methods of extraction could be considered as well and that the results presented in the following are only relevant to this method.

A. Comparison With THELMA

The THELMA code was developed to analyze the electromagnetic and thermo-hydraulic transients of superconducting CICCs for fusion magnets [21], [22]. In this work, the electromagnetic part of the code [23] is applied to the analysis of the CS ITER conductor, through the same 24-sub-cable model adopted for the analysis of AC losses in the CS Insert experiment [24].

We have agreed with the University of Bologna to compare the outputs of our modeling with those of THELMA on this representation of the last two stages of ITER CS conductor subject to a cyclic transverse and uniform magnetic excitation. The considered geometry was then a sextuplet of quadruplets, i.e., six bundles of four elements (with diameter of 6.49 mm) each, and the cycles were $+/-$ 0.2 T triangles with frequency set to 0.1 Hz. The effective parameters we have obtained following the method discussed previously are presented in Table I.

From these parameters we have then been able to compute the power dissipated by the coupling currents at the end of a ramp of the triangular magnetic excitation using (8) and (9) for constant $\dot{B}_a = 0.08$ T/s (i.e., steady-state regime for coupling currents). This calculation has led us to the following value of power per unit length of conductor: $P_l = 863$ mW.m^{-1}. We have found this value to be about 30% higher than the one computed by THELMA which was around 667 mW.m^{-1} (between 662 mW.m^{-1} and 673 mW.m^{-1} depending on the length of cable).

In addition, we have also computed the longitudinal current induced in the first element of the first bundle $I_{11}(z)$ and compared it with the one obtained by THELMA; the results are displayed on Fig. 2.

We can see on Fig. 2 the good agreement between the results of both models. The additional peaks and dips and the horizontal

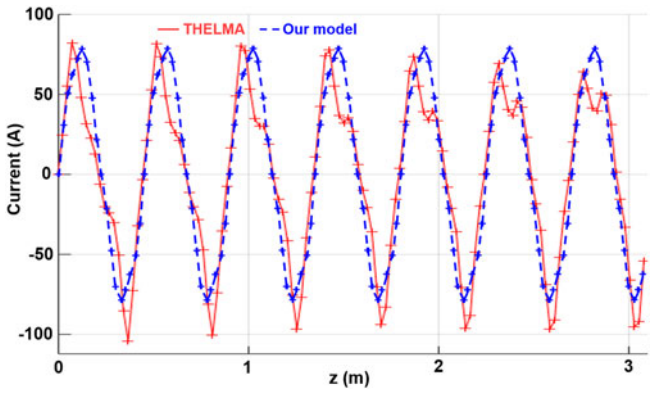

Fig. 2. Current induced in first element of first bundle along conductor axis.

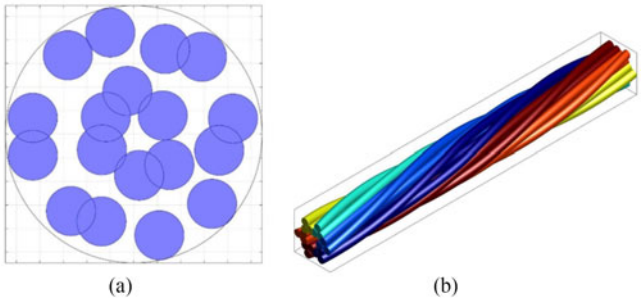

Fig. 3. Cross-section (a) and 3D geometry (b) produced by JACKPOT.

TABLE II
EFFECTIVE PARAMETERS EXTRACTED FROM JACKPOT DATA

Effective parameters	l_{p_k} (mm)	R_{c_k} (mm)	σ_{l_k} (10^7 S/m)
Substage ($k = 1$)	187.0	2.96	1.38
Superstage ($k = 2$)	290.2	6.56	5.92

asymmetry of the curve computed by THELMA are due to the variations of the local transverse conductances which are constant in our model (σ_{l_1} and σ_{l_2} are averages).

B. Comparison With JACKPOT

JACKPOT AC/DC is a numerical model developed at the University of Twente [25]. It is an electromagnetic and thermal model that describes the AC/DC performance of CICCs and joints at strand level detail [26]. This model is used to study effects of current distribution non-uniformity, optimization of cable patterns and ITER and DEMO conductor and joint stability [27].

We also present here the comparison we have carried out with the University of Twente on a simplified geometry of the last two stages of JT-60SA TF conductor: sextuplet of triplets of elements with diameter of 4.21 mm (see Fig. 3). The conductor was subject to a sinusoidal magnetic field with frequency and amplitude (peak field) set to 0.05 Hz and to 1 T respectively.

We have deduced the effective parameters of Table II using the method described at the beginning of Section III from the element trajectories and the conductance network generated by JACKPOT.

TABLE III
EFFECTIVE PARAMETERS OBTAINED FOR JT-60SA TFCS CONDUCTOR

Stage (k)	1	2	3	4	5
l_{p_k} (mm)	45.4	66.7	120.2	185.2	285.7
R_{c_k} (mm)	0.49	0.82	1.62	2.31	7.75

Using (8) and (9) for a slowly-time varying regime and the parameters of Table II, we have computed the coupling losses dissipated in a sinusoidal cycle and obtained the following value per unit length of conductor: $Q_l = 18.94$ J.m^{-1}/cycle. This value is about 40% higher than the one computed by JACKPOT, i.e., 13.35 J.m^{-1}/cycle.

C. Discussions

In order to understand the origin of the differences between both approaches, several numerical effects have been investigated (changes of spatial discretization, length of conductor and initial phase shifts between elements) but none of them were responsible for the 30–40% discrepancy.

In fact, for both tested geometries, the coupling power is almost exclusively due to the inter-bundle currents (i.e., superstage); the difference is then bound to come from considerations made at the superstage scale. In our approach, the local transverse voltages and conductances between any element of a bundle and any element of an adjacent bundle are all set to their respective average $U_{\rm avg}$ and $\sigma_{\rm avg}$. We then tend to underestimate the local transverse conductance $\sigma_{\rm loc}$ (compared to the one of JACKPOT or THELMA) and overestimate the local transverse voltage $U_{\rm loc}$ between close elements of adjacent bundles and vice versa for distant elements. The local power dissipated between elements of adjacent bundles being equal to $P_{\rm loc} = \sigma_{\rm loc} U_{\rm loc}^2$, it is legitimate to expect that the antagonistic effects cancel each other out so that the average power dissipated between adjacent bundles would be close to $P_{\rm avg} = \sigma_{\rm avg} U_{\rm avg}^2$. However $\sigma_{\rm loc}$, and thus $P_{\rm loc}$, are always zero between distant elements in THELMA and JACKPOT but this is not the case in our model. Consequently, using the method described at the beginning of Section III, we slightly overestimate the total power compared to numerical codes

IV. PARAMETERS EXTRACTED FROM X-RAY TOMOGRAPHY

In the framework of a collaboration with the INFLPR Bucharest, we have reconstructed the strand trajectories inside samples of a JT-60SA TF conductor from 2D transverse images obtained via X-ray tomography [28]. After having processed these trajectories, we have been able to extract the effective geometrical parameters of this conductor; they are presented in Table III and are in very good agreement with the cable geometrical specifications [29]. We are now planning to use inter-strand resistivity measurements of this conductor to deduce its effective electrical parameters. We would then be able to compare the losses computed with our analytical modeling with those measured within SULTAN facilities.

V. Conclusion and Prospects

Extending our previous studies on composites and on a group of twisted elements, we have been able to deal with the complexity inherent to the non-periodic geometry of a two cabling stage conductor. We have developed an analytical model of the coupling losses induced in any magnetic regime and have provided a derivation of (4) which hitherto constituted a heuristic assumption of MPAS. The fair agreement of our approach with two different numerical models on two different geometries has clearly demonstrated its trustworthiness, though it appears to be slightly conservative. We plan to keep investigating the origins of this effect, to explore different magnetic regimes and to consider other methods for the calculation of the effective parameters. Moreover, we have been able to extract the effective geometrical features of a real conductor; the next step will then be to deduce its effective conductances from inter-strand resistivity measurements in order to compare our results with real losses measurements. Finally, since we have been able to extend the analytical model of a one cabling stage conductor to a two cabling stages one, we are now investigating the possibility to find an iterative process to reach a higher number of cabling stages.

References

[1] M. N. Wilson, C. R. Walters, J. D. Lewin, P. F. Smith, and A. H. Spurway, "Experimental and theoretical studies of filamentary superconducting composites," *J. Phys. D, Appl. Phys.*, vol. 3, no. 11, pp. 1517–1585, Nov. 1970.

[2] G. H. Morgan, "Theoretical behavior of twisted multicore superconducting wire in a time-varying uniform magnetic field," *J. Appl. Phys.*, vol. 41, no. 9, pp. 3673–3679, Mar. 1970.

[3] W. J. Carr Jr., "Conductivity, permeability, and dielectric constant in a multifilament superconductor," *J. Appl. Phys.*, vol. 41, no. 9, pp. 3673–3679, Mar. 1970.

[4] G. Ries, "AC-losses in multifilamentary superconductors at technical frequencies," *IEEE Trans. Magn.*, vol. MAG-13, no. 1, pp. 524–526, Jan. 1977.

[5] W. J. Carr Jr., "Longitudinal and transverse field losses in multifilament superconductors," *IEEE Trans. Magn.*, vol. MAG-13, no. 1, pp. 129–136, Jan. 1977.

[6] J. P Soubeyrand and B. Turck, "Losses in superconducting composites under high rate pulsed field," *IEEE Trans. Magn.*, vol. 15, no. 1, pp. 248–251, Jan. 1979.

[7] B. Turck, "Coupling losses in various outer normal layers surrounding the filament bundle of a superconducting composite," *J. Appl. Phys.*, vol. 50, no. 8, pp. 5397–5401, Aug. 1979.

[8] A. M. Campbell, "A general treatment of losses in multifilamentary superconductors," *Cryogenics*, vol. 22, pp. 3–16, 1982.

[9] M. N. Wilson, "Time-varying fields and A.C. losses," in *Superconducting Magnets*. New York, NY, USA: Oxford Univ. Press, 1983, pp. 176–180.

[10] P. Tixador, "Supraconductivité," in *Les Supraconducteurs*. Paris, France: Editions Hermès, 1995, pp. 53–58.

[11] A. Nijhuis, H. H. J. ten Kate, P. L. Bruzzone, and L. Bottura, "Parametric study on coupling loss in subsize ITER Nb3Sn cabled specimens," *IEEE Trans. Magn.*, vol. 32, no. 32, pp. 2743–2746, Jul. 1996.

[12] H. H. J. ten Kate, "AC losses and magnet research," *Adv. Cryogenic Eng.*, vol. 40, pp. 559–568, 1994.

[13] A. Nijhuis, H. H. J. ten Kate, J. L. Duchateau, and P. L. Bruzzone, "Coupling loss time constant in full size Nb3Sn CIC model conductors for fusion magnets," *Adv. Cryogenic Eng.*, vol. 42B, pp. 1281–1288, 1996.

[14] P. L. Bruzzone, A. Nijhuis, and H. H. J. ten Kate, "Contact resistance and coupling loss in cable-in-conduit of Cr plated Nb3Sn strands," in *Proc. Int. Conf. MT-15*, Beijing, China, Oct. 1998. pp. 1295–1298.

[15] A. Nijhuis, Y. Ilyin, W. Abbas, B. ten Haken, and H. H. J. ten Kate, "Change of interstrand contact resistance and coupling loss in various ITER NbTi conductors with the transverse loading in the Twente Cryogenic Cable Press up to 40,000 cycles," *Cryogenics*, vol. 44, pp. 319–339, 2004.

[16] B. Turck and L. Zani, "A macroscopic model for coupling current losses in cables made of multistages of superconducting strands and its experimental validation," *Cryogenics*, vol. 50, pp. 443–449, 2010.

[17] A. Louzguiti, L. Zani, D. Ciazynski, B. Turck, and F. Topin, "Development of an analytical-oriented extensive model for AC coupling losses in multilayer superconducting composite," *IEEE Trans. Appl. Supercond.*, vol. 26, no. 3, Apr. 2016, Art. no. 4700905.

[18] A. Louzguiti *et al.*, "AC coupling losses in CICCs: Analytical modeling at different stages," *IEEE Trans. Appl. Supercond.*, vol. 27, no. 4, Jun. 2017, Art. no. 0600505.

[19] T. Schild and D. Ciazynski, "A model for calculating AC losses in multistage superconducting cables," *Cryogenics*, vol. 36, pp. 1039–1049, 1996.

[20] A. Louzguiti, "Magnetic screening currents and coupling losses induced in superconducting magnets for thermonuclear fusion," Ph.D. dissertation, Aix-Marseille Univ., Marseille, France, 2018.

[21] M. Ciotti, A. Nijhuis, P. L. Ribani, L. Savoldi Richard, and R. Zanino, "THELMA code electromagnetic model of ITER superconducting cables and application to the ENEA stability experiment," *Supercond. Sci. Technol.*, vol. 19, pp. 987–997, Oct. 2006.

[22] F. Bellina *et al.*, "Numerical analysis of the ITER TF conductor samples in SULTAN with the THELMA code," *IEEE Trans. Appl. Supercond.*, vol. 19, no. 3, pp. 1457–1461, Jun. 2009.

[23] M. Breschi and P. L. Ribani, "Electromagnetic modeling of the jacket in cable-in-conduit conductors," *IEEE Trans. Appl. Supercond.*, vol. 18, no. 1, pp. 18–28, Mar. 2008.

[24] M. Breschi *et al.*, "Analysis of AC losses in the ITER central solenoid insert coil," *IEEE Trans. Appl. Supercond.*, vol. 27, no. 4, Jun. 2017, Art. no. 4200605.

[25] E. P. van Lanen and A. Nijhuis, "JackPot: A novel model to study the influence of current non-uniformity and cabling patterns in cable-in-conduit conductor," *Cryogenics*, vol. 50, pp. 139–148, 2010.

[26] E. P. A. van Lanen, J. van Nugteren, and A. Nijhuis, "Validation of a strand level CICC-joint coupling loss model," *Supercond. Sci. Technol.*, vol. 25, no. 2, 2012, Art. no. 025013.

[27] T. Bagni, M. Breschi, J. Duchateau, A. Devred, and A. Nijhuis, "Analysis of ITER Nb-Ti and Nb3Sn CICCs experimental minimum quench energy with jackpot, MCM and THEA models," *Supercond. Sci. Technol.*, vol. 30, no. 9, 2017, Art. no. 095003.

[28] I. Tiseanu, L. Zani, C. Tiseanu, T. Craciunescu, and C. Dobrea, "Accurate 3D modeling of cable in conduit conductor type superconductors by X-ray microtomography," *Fusion Eng. Des.*, vol. 98/99, pp. 1176–1180, 2015.

[29] L. Zani *et al.*, "Design of JT-60SA magnets and associated experimental validations," *IEEE Trans. Appl. Supercond.*, vol. 21, no. 3, pp. 1938–1943, Jun. 2011.